

Nonlinear Susceptibility in Semiconductor hetrostructures

Mohsin K. Al-khaykanee

College of Science\ University of Babylon

Introduction

The linear and non-linear optical properties of three-level systems get a great importance from both theoretical and experimental points of view. This is due to the phenomena related to these systems, like electromagnetic induced transparency (EIT), coherent population trapping (CPT) and coherent adiabatic population (CAP) [1]. In contrast to CPT which is a “spectroscopic” phenomenon that involves only modifications to the material states in an optically thin sample, EIT is a phenomenon specific to optically thick media where both the optical fields and the material states are modified [2]. The importance of EIT stems from the fact that it gives rise to greatly enhance non-linear susceptibility in the spectral region of induced transparency of the medium and is associated with steep dispersion.

In all these processes, the three-level atomic systems are in the form of either three schemes [1]: (a) a ladder or cascade system ($E_1 < E_2 < E_3$); (b) a L scheme ($E_1 < E_3 < E_2$); (c) a V scheme ($E_2 < E_1$ and E_3), see Fig. 1. Third-order non-linear susceptibility ($\chi^{(3)}$) in a three-level atomic system is discussed extensively in the literature. For example, ($\chi^{(3)}$) for EIT in L scheme is discussed in [1] and [3] for the threelevel atoms coupled to the applied laser fields and determines the optical response. Susceptibility in CPT is discussed in [3]. Recently, EIT takes an additional importance due to important applications like slow-light, where a solution to several challenging problems in various engineering applications is introduced. This includes optical delay lines or optical buffers, low-light level non-linear optical devices, optical pulse synchronization and reshaping, all-optical signal, quantum information processing, and miniaturization of many spectroscopy systems due to the availability of a variable delay line [4].

It is predicted that QDs have excellent linear and non-linear properties mainly due to discrete electronic energy states which result from three-dimensional confinement making it a good candidate for most optoelectronic applications including three-level system applications [5]. Our analysis is based on the one-particle density matrix formalism taking into account the intersubband relaxation. This paper is organized as follows: Section 2 includes the third-order non-linearity derivation; Section 3 includes calculations, results and discussion of the third-order non-linear intersubband absorption in a three-level semiconductor QDs from the corresponding susceptibility, where structures of different QD

sizes are studied. Structures with different WL compositions are also included in this study. The study examines the effect of homogeneous linewidths and the damping rates. Section 4 includes brief conclusions from this study.

Theoretical model of nonlinear susceptibility

There are many ways to represent a three-level system in semiconductor structures. A simple threelevel ladder system is physically constructed here by an InGaAs-QD “active” region, see Fig. 1 (d). The signal beam ν_s is connecting between C1 (j_{1i} state (and HH1 (j_{2i} state) while the pump beam ν_p is the control beam connecting between C1 and C2 (j_{3i} state). Uniform QD structure is assumed here. A description of the QD system used in the calculations is found in Appendix A. As a result of the coherent coupling between the atomic system and the laser beams, atomic levels are no longer eigenstates of the system. Instead, they are dressed by the pump laser and become two new states j_{2di} and j_{3di} , Fig. 1 (d). This (destructive) quantum interference between two absorption paths produces a transparency spectral window in the middle of the strong j_{1i} to j_{2i} absorption line. The width of this transparency window is strongly dependent on the intensity of the pump light field. The time-dependent optical dielectric constant experienced by the signal (s) and the pump (p) beams can be derived from the equation of motion for the density matrix as follows:

$$\frac{\partial}{\partial t} \rho_{uv} = -(i\omega_{uv} + \gamma_{uv})\rho_{uv} - \frac{i}{\hbar} [\hat{V}, \hat{\rho}]_{uv} \quad (1)$$

$$\hat{V}_{uv} = -\frac{1}{2} \mu_{uv} E(\omega) + c.c., \quad (2)$$

Where γ_{uv} is the dephasing linewidth, and ω_{uv} is energy separation between states $|n\rangle$ and $|m\rangle$. μ_{uv} is the dipole moment. The electric field $E(\omega)$ includes the signal and pump beams, so it is expressed as [47]

$$E(\omega) = E_s e^{-i\omega_s t} + E_p e^{-i\omega_p t} \quad (3)$$

We derive the third-order non-linear intersubband absorption coefficient $\alpha^{(3)}(\omega_s, \omega_p)$ in a three level system. Thus, we must derive $\rho_{\sim 21}^{(3)}$. This third order term is composed of the three modes s, p, and q, i.e.

$$\rho_{\sim 21}^{(3)} = \sum_{s,p,q \sim 21} \rho^{(3)}(s,p,q) \quad (4)$$

The component $\rho_{\sim 21}^{(3)}(S,P,Q)$ has the phase rotations $\exp[i(\pm\omega_s \mp \omega_p + \omega_q)t]$ For the case of two modes propagating [7]:

$$\rho_{\sim 21}^{(3)}(s,p,p) = \left[\rho_{21}^{(3)}(-\omega_s + \omega_p - \omega_p) + \rho_{21}^{(3)}(-\omega_p + \omega_p - \omega_s) + \rho_{21}^{(3)}(\omega_p - \omega_p - \omega_s) + \rho_{21}^{(3)}(\omega_p - \omega_s - \omega_p) \right] e^{-i\omega_s t} \quad (5)$$

To get the 1st and 2nd terms of Eq. (2), we apply the density matrix,

$$\frac{\partial}{\partial t} \left[\rho_{\sim 21}^{(3)}(-\omega_s + \omega_p - \omega_p) e^{-i(\omega_s - \omega_p + \omega_p)t} + \rho_{\sim 21}^{(3)}(-\omega_p + \omega_p - \omega_s) e^{-i(\omega_p - \omega_p + \omega_s)t} \right] \quad (6)$$

$$= [-i\omega_{21} - \gamma_{21}] \rho_{\sim 21}^{(3)} - \frac{1}{2i\hbar} \left[\mu_{21} (\rho_{11}^{(2)} - \rho_{22}^{(2)}) + \mu_{23} \rho_{31}^{(2)} \right] E(t)$$

The slowly varying density matrices σ_{ij} are defined as follows:

$$\begin{aligned} \rho_{21}(t) &= \sigma_{21}(t) e^{-i\omega_s t}, \\ \rho_{32}(t) &= \sigma_{32}(t) e^{-i\omega_p t}, \\ \rho_{31}(t) &= \sigma_{31}(t) e^{-i(\omega_s + \omega_p)t} \end{aligned} \quad (7)$$

This gives

$$\begin{aligned} & [i(\omega_{21} - \omega_s) + \gamma_{21}] \left[\rho_{\sim 21}^{(3)}(-\omega_s + \omega_p - \omega_p) + \rho_{\sim 21}^{(3)}(-\omega_p + \omega_p - \omega_s) \right] e^{-i\omega_s t} \\ &= -\frac{\mu_{21}}{2i\hbar} \left[\sigma_{11}^{(2)}(\omega_s - \omega_p) e^{-i(\omega_s - \omega_p)t} E_p e^{-i\omega_p t} - \sigma_{22}^{(2)}(\omega_s - \omega_p) e^{-i(\omega_s - \omega_p)t} E_p e^{-i\omega_p t} \right] \quad (8) \\ & -\frac{\mu_{21}}{2i\hbar} \left[\sigma_{11}^{(2)}(-\omega_p + \omega_p) e^{-i(\omega_p - \omega_p)t} E_s e^{-i\omega_s t} - \sigma_{22}^{(2)}(-\omega_p + \omega_p) e^{-i(\omega_p - \omega_p)t} E_s e^{-i\omega_s t} \right] \end{aligned}$$

$\sigma_{11}^{(2)}$ and $\sigma_{22}^{(2)}$ are derived. The 3rd and 4th terms in Eq. (2) are similar to those in the 1st and 2nd terms. The summation of all these terms gives $\sigma_{21}^{(3)}(s, p, p)$. Collecting these terms gives

$$\begin{aligned} \sigma_{21}^{(3)}(s, p, p) &= \frac{|\mu_{21}|^2 E_p^*}{2i\hbar^2} \frac{\Omega_s (\rho_{11}^{(0)} - \rho_{22}^{(0)}) E_p}{(\tilde{\gamma}_{21})^2 \left[1 + |\Omega_p|^2 / \tilde{\gamma}_{21} \tilde{\gamma}_{31} \right]} \left[\frac{1}{[i(\omega_p - \omega_s) + \gamma_{11}] + \gamma_{11}} + \frac{1}{\gamma_{11}} \right] + \frac{\mu_{21} E_p}{2i\hbar^2 \tilde{\gamma}_{21}} \\ & * \left[\frac{\mu_{21} \Omega_s (\rho_{11}^{(0)} - \rho_{22}^{(0)}) E_p^*}{\tilde{\gamma}_{21} \left[1 + |\Omega_p|^2 / \tilde{\gamma}_{21} \tilde{\gamma}_{31} \right]} - (\mu_{32} \frac{E_s}{\tilde{\gamma}_{23}}) \left\{ \Omega_p^* (\rho_{33}^{(0)} - \rho_{22}^{(0)}) - \frac{|\Omega_s|^2 \Omega_p^* (\rho_{11}^{(0)} - \rho_{22}^{(0)})}{\tilde{\gamma}_{13} \tilde{\gamma}_{12} \left[1 - |\Omega_p|^2 / \tilde{\gamma}_{13} \tilde{\gamma}_{12} \right]} \right\} \right] \\ & * \left[\frac{1}{[i(\omega_p - \omega_s) + \gamma_{22}] + \gamma_{22}} \right] \end{aligned} \quad (9)$$

Where $\Delta_s = \omega_{21} - \omega_s$ and $\Delta_p = \omega_{32} - \omega_p$ are detunings from the signal and pump beams, respectively. The complex detunings are $\tilde{\gamma}_{12} = \gamma_{12} - i\Delta_s$ and $\tilde{\gamma}_{13} = \gamma_{13} - i(\Delta_s + \Delta_p)$. The definition of Rabi frequency is $\Omega = \mu E / 2\hbar$. For the third-order susceptibility (in a three-level system) we have

$$\alpha^{(3)}(\omega_s, \omega_p) = -\frac{6 \omega_s}{5 n_r} \sqrt{\frac{\mu}{\epsilon_0}} \frac{|\mu_{21}|^2}{2\hbar^2 V} \frac{1}{1 + \delta_{sp}} \operatorname{Re} \left\{ \frac{|\mu_{21}|^2 (\rho_{11}^{(0)} - \rho_{22}^{(0)})}{\hbar (\tilde{\gamma}_{21})^2 (1 + |\Omega_p|^2 / \tilde{\gamma}_{21} \tilde{\gamma}_{31})} \left[\frac{1}{[i(\omega_p - \omega_s) + \gamma_{11}] + \gamma_{11}} + \frac{1}{\gamma_{11}} \right] \right. \\ \left. + \frac{2}{\tilde{\gamma}_{21}} \left[\frac{|\mu_{21}|^2 (\rho_{11}^{(0)} - \rho_{22}^{(0)})}{2\hbar \tilde{\gamma}_{21} [1 + |\Omega_p|^2 / \tilde{\gamma}_{21} \tilde{\gamma}_{31}]} - \frac{|\mu_{32}|^2}{2\hbar \tilde{\gamma}_{23}} (\rho_{33}^{(0)} - \rho_{22}^{(0)}) \right] * \left[\frac{1}{[i(\omega_p - \omega_s) + \gamma_{22}] + \gamma_{22}} + \frac{1}{\gamma_{22}} \right] \right\}$$

(10)

Note that V is the QD volume, Γ is the optical confinement factor and $\delta_{sp} = 1$ for $s=p$ and $\delta_{sp} = 0$ for $s \neq p$. For the linear susceptibility in three-level system we have [8]

$$\epsilon_0 \chi^{(1)}(\omega_s) = -i \frac{|\mu_{21}|^2}{V \hbar} \frac{(\rho_{22} - \rho_{11})}{\tilde{\gamma}_{21} [1 + (|\Omega_p|^2 / \tilde{\gamma}_{21} \tilde{\gamma}_{31})]} \quad (11)$$

The absorption coefficient $\alpha^{(3)}(\omega_s, \omega_p)$ is defined as

$$\alpha^{(3)}(\omega_s, \omega_p) = \frac{\omega_s}{n_r} \sqrt{\frac{\mu}{\epsilon_0}} \operatorname{Im}(\epsilon_0 \chi^{(3)}(\omega_s, \omega_p)) \quad (12)$$

Then from (10) and (12) the third-order non-linear absorption in a three-level system is

$$\alpha^{(3)}(\omega_s, \omega_p) = -\frac{6 \omega_s}{5 n_r} \sqrt{\frac{\mu}{\epsilon_0}} \frac{|\mu_{21}|^2}{2\hbar^2 V} \frac{1}{1 + \delta_{sp}} \operatorname{Re} \left\{ \frac{|\mu_{21}|^2 (\rho_{11}^{(0)} - \rho_{22}^{(0)})}{\hbar (\tilde{\gamma}_{21})^2 (1 + |\Omega_p|^2 / \tilde{\gamma}_{21} \tilde{\gamma}_{31})} \left[\frac{1}{[i(\omega_p - \omega_s) + \gamma_{11}] + \gamma_{11}} + \frac{1}{\gamma_{11}} \right] \right. \\ \left. + \frac{2}{\tilde{\gamma}_{21}} \left[\frac{|\mu_{21}|^2 (\rho_{11}^{(0)} - \rho_{22}^{(0)})}{2\hbar \tilde{\gamma}_{21} [1 + |\Omega_p|^2 / \tilde{\gamma}_{21} \tilde{\gamma}_{31}]} - \frac{|\mu_{32}|^2}{2\hbar \tilde{\gamma}_{23}} (\rho_{33}^{(0)} - \rho_{22}^{(0)}) \right] * \left[\frac{1}{[i(\omega_p - \omega_s) + \gamma_{22}] + \gamma_{22}} + \frac{1}{\gamma_{22}} \right] \right\}$$

(13)

The total absorption coefficient is given by

$$\alpha(\omega_s, I_p) = \alpha^{(1)}(\omega_s, I_p) + \alpha^{(3)}(\omega_s, I_p) \quad (14)$$

Calculations, Results and Discussion

The structures that used in study nonlinear susceptibility was sizes several and increasing Ga mole–fraction in WL. We present the results by following the absorption dependence on (1) pump power density, (2) radius and height of the QD, and (3) the interband and intersubband transitions. We study the intersubband non–linear absorption spectra in a QD as a function of the photon energy. We present the results by following the absorption dependence on (1) pump power density, (2) radius and height of the QD and (3) the interband and intersubband transitions.

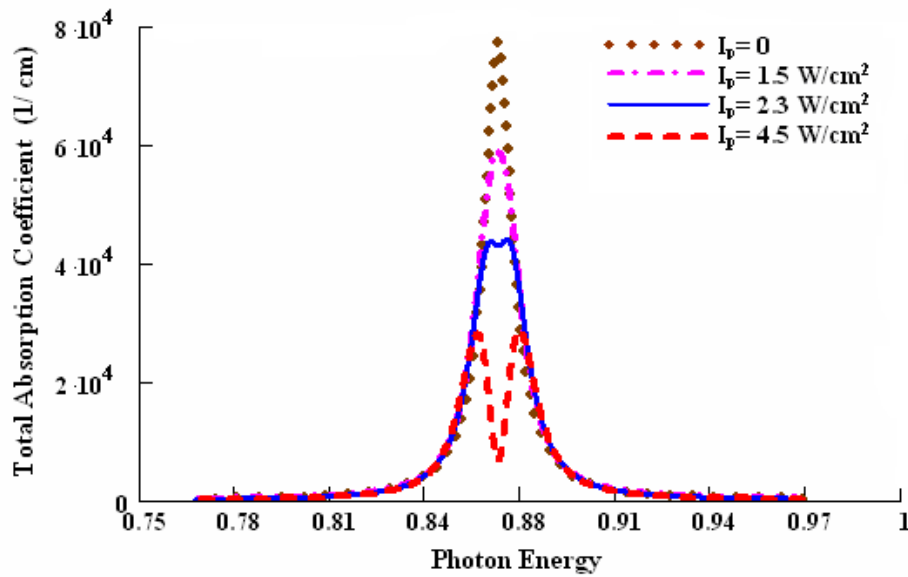


Figure 1: Intersubband total absorption coefficient $\alpha(\omega_s, I_p)$ versus photon energy $\hbar\omega_s$ for a QD of a radius $a = 14 \text{ nm}$, height $h = 3.5 \text{ nm}$ and with interband dipole moment $5.1e \text{ \AA}$ with carrier density $1.84 \times 10^{18} / \text{cm}^3$ at three different optical intensities: (i) $I_p = 0$, (ii) $I_p = 1.5 \text{ W/cm}^2$, (iii) $I_p = 2.3 \text{ W/cm}^2$, (iiii) $I_p = 4.5 \text{ W/cm}^2$.

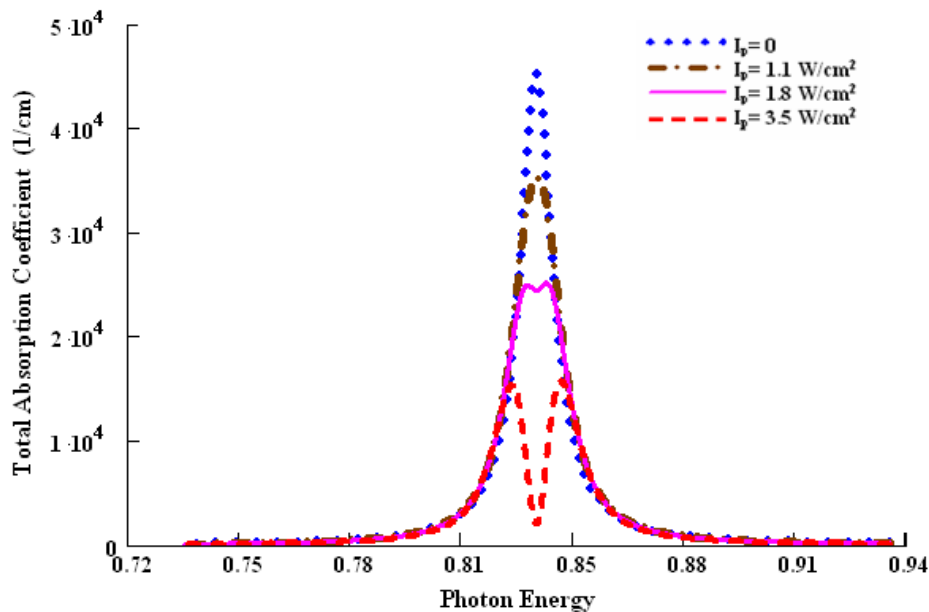


Figure 2: Intersubband total absorption coefficient $\alpha(\omega_s, I_p)$ versus photon energy $\hbar\omega_s$ for a quantum dot (QD) of a radius $a = 14$ nm, height $h = 6.5$ nm and with interband dipole moment 5.5 eÅ with carrier density 1.84×10^{18} /cm³ plotted at three different optical intensities : (i) $I_p = 0$, (ii) $I_p = 1.1$ W/cm², (iii) $I_p = 1.8$ W/cm², (iiii) $I_p = 3.5$ W/cm².

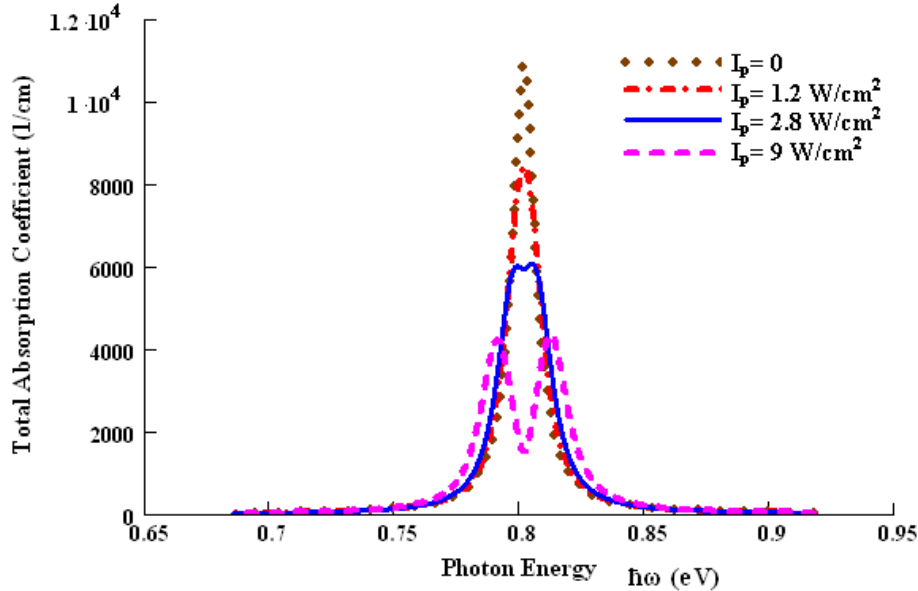


Figure 3: Intersubband total absorption coefficient $\alpha(\omega_s, I_p)$ versus photon energy $\hbar\omega$ for a quantum dot (QD) of a radius $a = 14$ nm, height $h = 28$ nm and with interband dipole moment 6.03 eÅ with 1.84×10^{18} /cm³ electrons with zero electric field is plotted three different optical intensities : (i) $I_p = 0$, (ii) $I_p = 1.2$ W/cm², (iii) $I_p = 2.7$ W/cm², (iiii) $I_p = 9$ W/cm².

The total absorption coefficient $\alpha(\omega_s, I_p)$ as a function of the signal detuning at various optical intensities, for $\text{In}_{.5}\text{Ga}_{.5}\text{As}/\text{In}_{.9}\text{Ga}_{.1}\text{As}_{.78}\text{P}_{.21}$ QD structure (structure No. 2) is shown in Fig. 2 (a) where the spectral hole appears at $I_p = 6$ W/cm². Fig. 2 (b) shows the absorption coefficient $\alpha(\omega_s, I_p)$ for $\text{In}_{.5}\text{Ga}_{.5}\text{As}/\text{In}_{.8}\text{Ga}_{.2}\text{As}_{.77}\text{P}_{.22}$ QD structure (structure No. 10) where the spectral hole becomes to appear at $I_p = 5$ W/cm². Fig.2 (c) shows the absorption coefficient $\alpha(\omega_s, I_p)$ for $\text{In}_{.5}\text{Ga}_{.5}\text{As}/\text{In}_{.61}\text{Ga}_{.39}\text{As}_{.17}\text{P}_{.83}$. In Fig. 2 (c), the spectral hole appears at $I_p = 4.1$ W/cm². Here, the spectral hole began to appear at low power

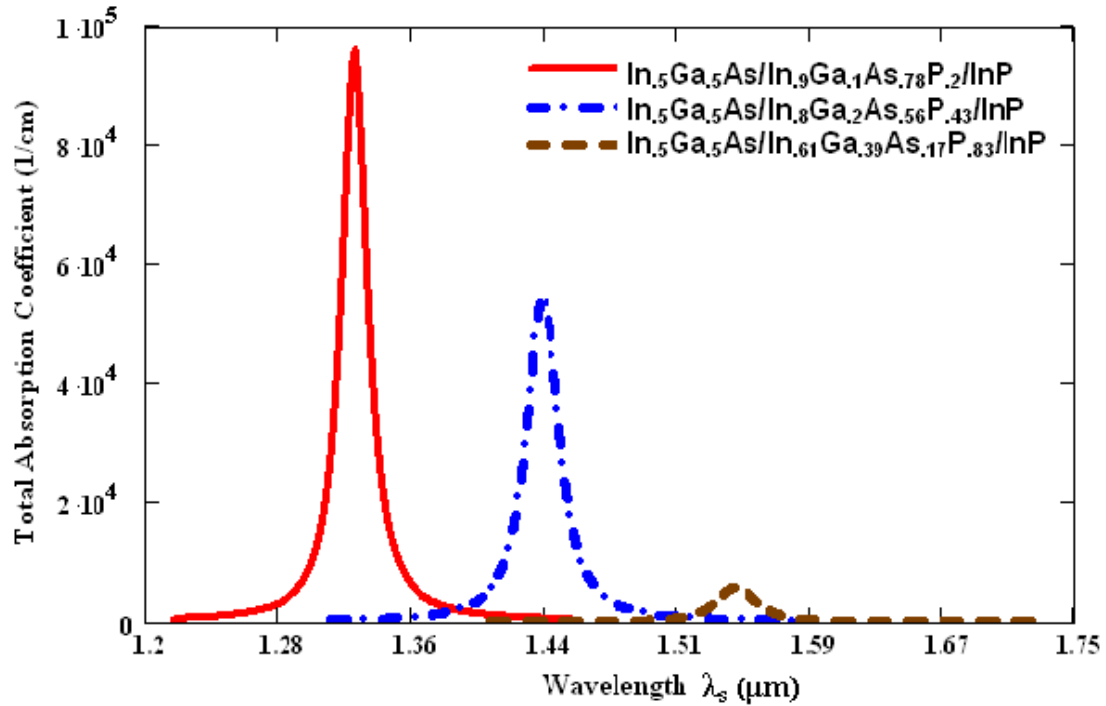
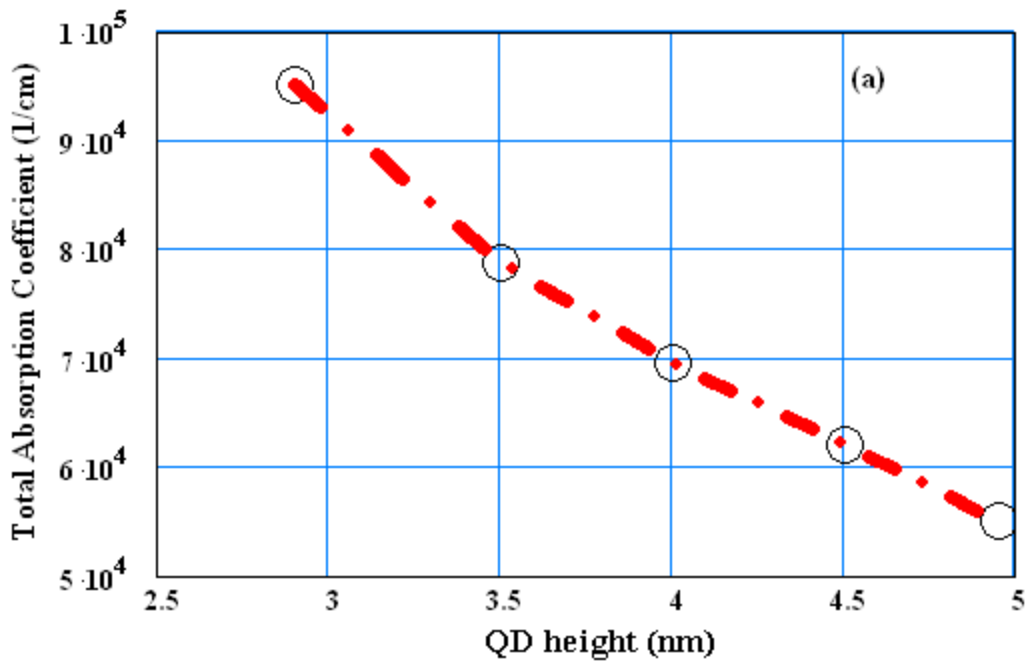


Figure 4: Intersubband total absorption coefficient $\alpha(\omega_s, I_p)$ as function of signal wavelength λ_s at $I_p = 0$ for the structures $x = 0.1$, $x = 0.2$, and $x = 0.39$.

Fig. 5 (a) and (b) shows the total absorption coefficient $\alpha(\omega_s, I_p)$ as function of the size and radius of QD for InGaAs/ In_{0.9}Ga_{0.1}As_{0.78}P_{0.21} structure. The total absorption coefficient is shown to increase with reducing size (radius or height).



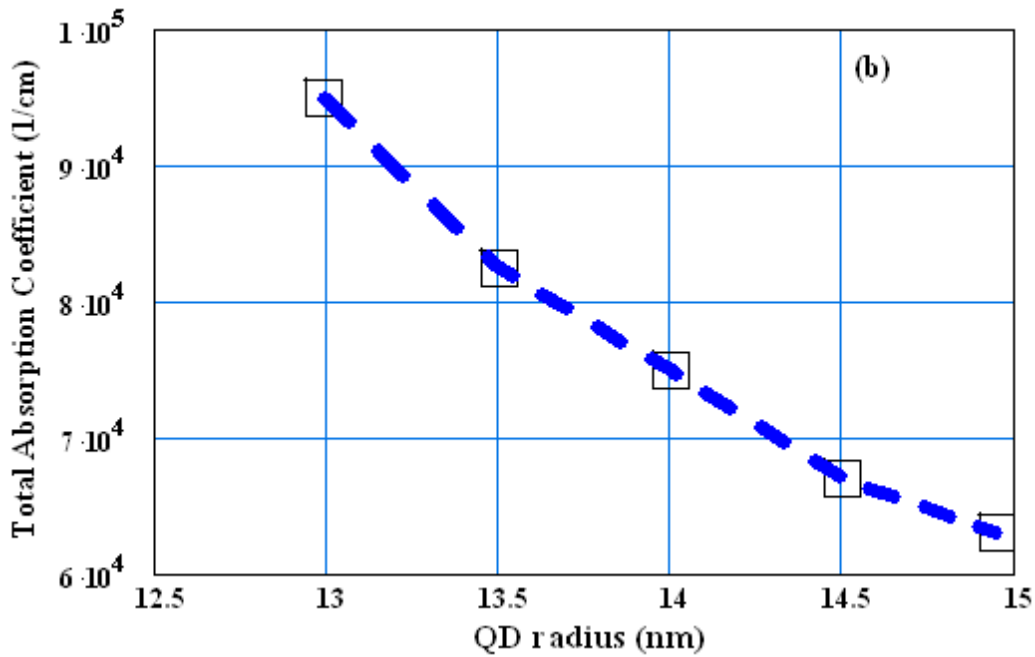
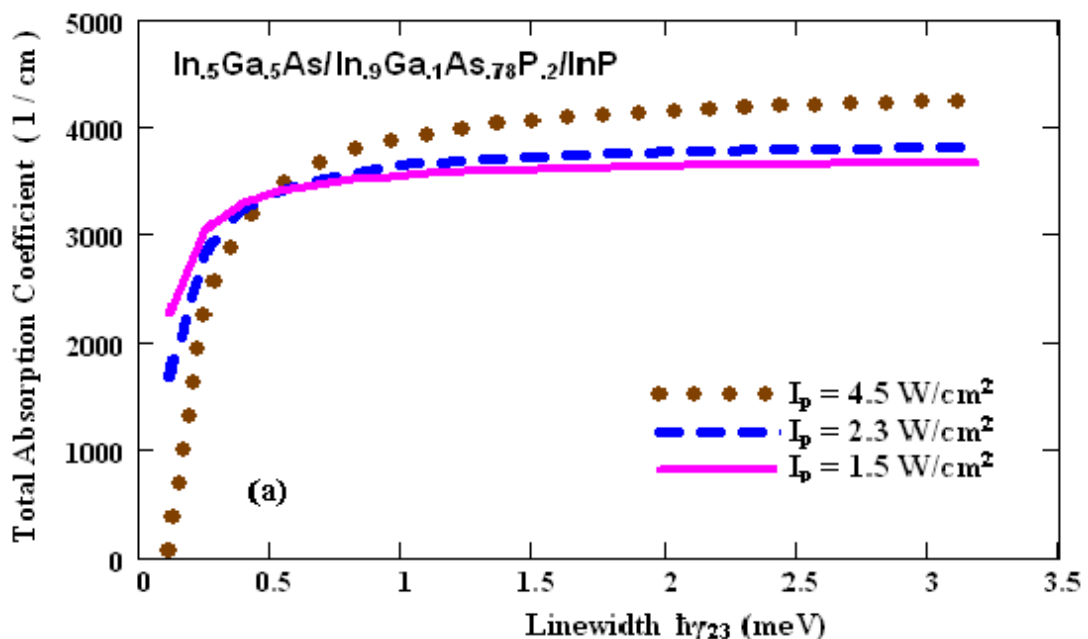


Figure 5: Absolute values of the total absorption coefficients $\alpha(\omega_s, I_p)$ as functions of the QD sizes (a) height, and (b) radius QD.

Fig. 6 (a) shows the total absorption coefficient for InGaAs/InGaAsP QD structure as a function of linewidth (γ_{23}) at different pumping powers. First, the total absorption reduced with increasing power then, an inversion occurs at 0.5 meV, where the total absorption increases with pumping. This figure also shows the secondary importance of this linewidth (γ_{23}). After 0.5 meV, total absorption is saturated. This behavior is also shown for other structures in Fig. 5 (b).



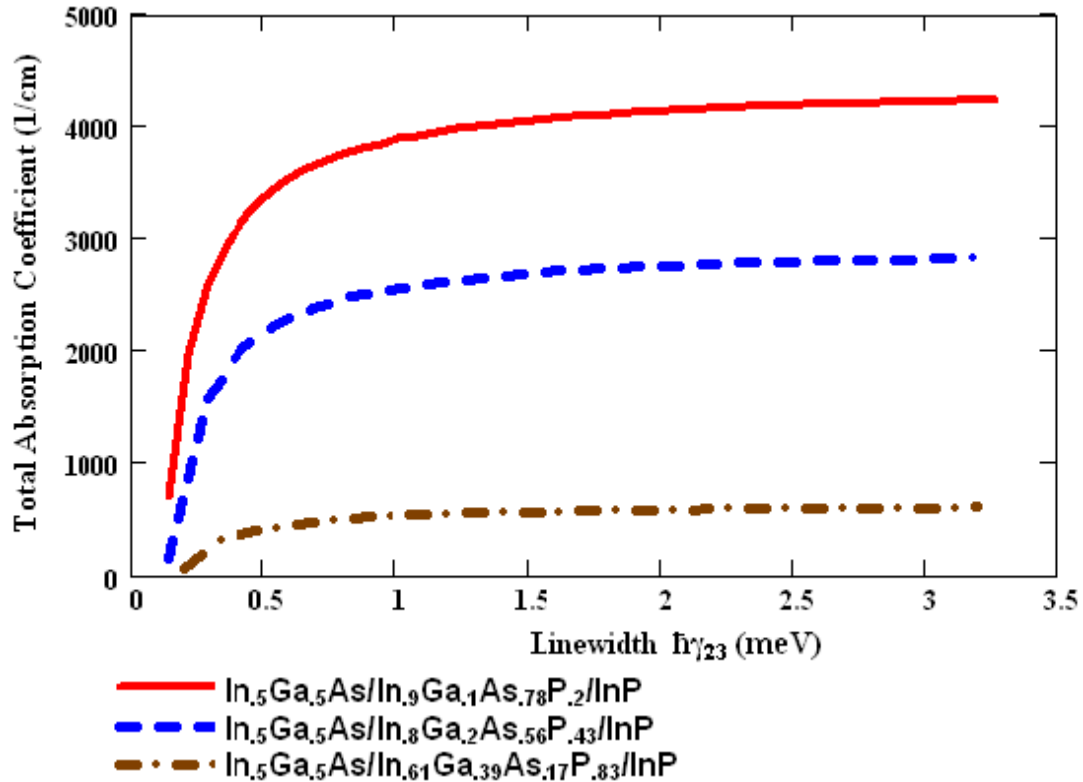


Figure 6: Total absorption coefficient $\alpha(\omega_s, I_p)$ versus damping rate γ_{23} at (a) pump power densities 4.5, 2.3, and 1.5 W/cm², for the structure $x = 0.1$, (b) $I_p = 4.5$ W/cm² for the structures $x = 0.1$, $x = 0.2$, and $x = 0.39$.

With increasing Ga mole-fraction in WL. Also, we check the beginning of spectral hole for the structures with other sizes in Table 1 (figures not shown here). We found that at smaller sizes the hole appears at a higher intensity. Thus, appearance of the spectral hole in structure No. 11 at low power relates, as a part, to longer size of this structure. It is also shown that the highest the optical beam intensity is, the smaller the value of the total absorption. This is due to the fact that the linear absorption coefficient is positive, and the non-linear absorption coefficient is negative. Fig. 3 shows the signal peaks for the three structures for clarity where one works at 1.3, 1.43 and 1.55 mm where the first and last ones are of considerable importance in optical communications. One can see from Fig. 2 that with increasing emission wavelength, the power required for the spectral hole to appear is reduced. Fig. 2 can be compared with the results in [9], who also found that the bigger the optical beam intensity is, the smaller the values of the total absorption.

Conclusions

Third-order non-linear susceptibility is derived for three-level quantum dot system. This is important in many non-linear applications for example electromagnetic induced transparency applications. InGaAs/ InGaAsP/InP system is taken as an example. The dephasing linewidth is shown to be of less importance.

References

- [1] E. Arimondo, in: E. Wolf (Ed.), Progress in Optics, vol. 35, Elsevier, Amsterdam, 1996, p. 257.
- [2] G.S. Agarwal, Microscopic approach to coherent population trapping state and its relaxation in a dense medium, Opt. Express 1 (1997) 44–48.
- [3] F. Renzoni, W. Maichen, L. Windholz and E. Arimondo, Coherent Population Trapping with Losses on the Sodium D1 Line Hanle Effect, <http://arxiv.org/abs/physics/9611007v1> [physics.atom-ph] 10 November 1996.
- [4] P.C. Ku, C.J. Chang–Hasnain, S.L. Chuang, Slow light in semiconductor heterostructures, J. Phys. D: Appl. Phys. 40 (2007) R93–R107.
- [5] M. Gioannini, A.H. Al–Khursan, G.A. The´, I. Montrosset, Simulation of quantum dot lasers with weak external optical feedback, in: Dynamics Days Conference, Delft–Netherlands, 2008.
- [6] M. Sugauara (Ed.), Self assembled InGaAs/GaAs quantum dots, Academic Press, 1999.
- [7] M. Yamada, Y. Suematsu, Analysis of gain suppression in undoped injection lasers, J. Appl. Phys. 52 (1981) 2653–2664.
- [8] C.J. Chang–Hasnain, P.C. Ku, J. Kim, S.L. Chuang, Variable optical buffer using slow light in semiconductor nanostructures, Proc. of IEEE 91 (2003) 1884–1896.
- [9] W.U. Bin–He, Transient intersubband optical absorption in double quantum well structure, Commun. Theor. Phys. (Beijing, China) 43 (2005) 759–764.
- [10] S.M. Ma, J.T. Seo, Q. Yang, R. Battle, H. Brown, K. Lee, L. Creekmore, A. Jackson, T. Skyles, B. Tabibi, S.S. Jung, W. Yu, M. Namkung, Third–order nonlinear susceptibility and hyperpolarizability of CdSe nanocrystals with femtosecond excitation, J. Korean Phys. Soc. 48 (2006) 1379–1384.